HHS Public Access

Author manuscript

IEEE J Biomed Health Inform. Author manuscript; available in PMC 2017 September 07.

Published in final edited form as:

IEEE J Biomed Health Inform. 2017 September ; 21(5): 1460–1465. doi:10.1109/JBHI.2016.2603159.

Movements indicate threat response phases in children at-risk for anxiety

Ellen W. McGinnis[*],
Department of Psychology, University of Michigan, Ann Arbor, MI USA

Ryan S. McGinnis[*] **[Member, IEEE]**,
Department of Mechanical Engineering, University of Michigan, Ann Arbor, MI USA and is now with the Department of Electrical and Biomedical Engineering, University of Vermont, Burlington, VT USA

Maria Muzik,
Department of Psychiatry, University of Michigan, Ann Arbor, MI USA

Jessica Hruschak,
Department of Psychiatry, University of Michigan, Ann Arbor, MI USA

Nestor L. Lopez-Duran,
Department of Psychology, University of Michigan, Ann Arbor, MI USA

Noel C. Perkins,
Department of Mechanical Engineering, University of Michigan, Ann Arbor, MI USA

Kate Fitzgerald, and
Department of Psychiatry, University of Michigan, Ann Arbor, MI USA

Katherine L. Rosenblum
Department of Psychiatry, University of Michigan, Ann Arbor, MI USA

Abstract

Temporal phases of threat response including Potential Threat (Anxiety), Acute Threat (Startle, Fear), and Post-threat Response Modulation have been identified as underlying markers of anxiety disorders. Objective measures of response during these phases may help identify children at risk for anxiety, however the complexity of current assessment techniques prevent their adoption in many research and clinical contexts. We propose an alternative technology, an inertial measurement unit (IMU), that enables non-invasive measurement of the movements associated with threat response, and test its ability to detect threat response phases in young children at heightened risk for developing anxiety. We quantified the motion of 18 children (3–7 years old) during an anxiety/fear provoking behavioural task using an IMU. Specifically, measurements from a single IMU secured to the child's waist were used to extract root-mean-square acceleration and angular velocity in the horizontal and vertical directions, and tilt and yaw range-of-motion during each threat response phase. IMU measurements detected expected differences in child motion by threat phase. Additionally, potential threat motion was positively correlated to familial anxiety

[*]Denotes collaborative first authors.

risk, startle range of motion was positively correlated with child internalizing symptoms, and response modulation motion was negatively correlated to familial anxiety risk. Results suggest differential theory-driven threat response phases, and support previous literature connecting maternal child risk to anxiety with behavioural measures using more feasible objective methods. This is the first study demonstrating the utility of an IMU for characterizing the motion of young children to mark the phases of threat response modulation. The technique provides a novel and objective measure of threat response for mental health researchers.

Index Terms

Mental Health; Inertial Sensors; Wearable Sensors; Child Anxiety; Fear

I. Introduction

Child anxiety is a widespread problem with studies showing that by age 12, up to 41% of children have experienced an anxiety disorder [1]. Early identification of these disorders improves the efficacy of intervention efforts [2]. Unfortunately, children under age 8 are not reliable reporters of their own anxiety [3], which leaves symptom reporting up to parents. However, parental report of child emotional problems are often inaccurate (i.e. [4]). Thus, researchers have looked to elicit observable markers of child anxiety using minimal-risk threat induction tasks to ultimately improve the reliability of anxiety assessment. Specifically, response to potential threat (anxiety), initial response to a known threat (startle response) [5] and “response modulation” (tempering the initial response) [6], have been identified as underlying markers of risk for anxiety disorders [7]–[9]. However, research is still limited by the scarcity of standardized, objective assessments for anxiety-relevant constructs in young children.

Objective assessments of child threat response phases currently include behavioral coding and physiological measures of startle including eye blink and muscle contraction. Child behaviors [10] are coded for anxiety and fear during standardized threat tasks, but these constructs are often referred to interchangeably [10]–[12]. While this aggregate fear/anxiety construct has been linked to familial risk for internalizing disorders in young children (e.g., [13]) and parent-reported child fear and internalizing symptoms [14], it does not discriminate the three distinct threat phases. Similarly, the startle phase is commonly measured using the Fear Potentiated Startle (FPS) technique, where electrodes quantify muscle activity during unpleasant stimuli [8], but this technique cannot be used to assess the other phases of threat response. With that said, eye blinks (i.e., small muscle contractions) have been related to child anxiety risk [8], and elevated child anxiety symptoms [7]. However, one study demonstrated that muscle group contractions were also significantly enlarged in children with anxiety compared to controls, suggesting measurement of full body motion may be used to examine initial threat response [9].

While these methodologies can detect threat phase data and predict anxiety risk, their use remains challenging due to personnel, time, expense, and data fidelity (e.g., 38% of FPS data are unusable due to child fidgeting [8]) issues. Moreover, their complexity hinders eventual

translation to clinical applications. Therefore, there is significant motivation to find a measure that reduces these barriers while providing sufficient sensitivity to expose the links between potential threat, startle, and response modulation behaviors and anxiety risk.

To this end, we propose the use of an inertial measurement unit (IMU) for measuring child motion quickly and inexpensively during clinical mood induction tasks. The IMU provides direct measurement of the full six degree-of-freedom motion of any body segment to which it is attached [15], [16], and can therefore be used for characterizing child behavior in a variety of contexts. Our hypothesis is that data from an IMU can be used to quantify the nuanced child behaviors inherent to the temporal threat response phases. Herein, we test this hypothesis by examining the relationship between movement parameters extracted from IMU data and the temporal constructs of threat response in a sample at heightened risk for developing anxiety: children of parents with post-traumatic stress disorder (PTSD) [17], and children with elevated internalizing symptoms [18].

II. Methods

A. Participants

Participants included 18 children (13 male) aged 3–7 years (M: 5.68, SD: 1.03) and their primary caregivers (16 mothers). Participants were recruited from a prior study (Maternal Anxiety During the Childbearing Years, PI: Muzik) of mothers with PTSD and from flyers in the community/psychiatry/psychology clinics. Thus, 47% of caregivers had a diagnosis of PTSD. Studies had approval from the University of Michigan Institutional Review Board (HUM00091788; HUM00033838). At-risk children were over-recruited in order to compare objective assessments to a wide range of symptomatology.

B. Protocol

The child and caregiver were brought into the university-based laboratory and consented to complete a videotaped threat response task with an IMU secured to the child's waist. Meanwhile, the caregiver completed multiple self-report questionnaires. Parents, but not children, were informed of the Snake Task to ensure a novel reaction from each child.

C. Measures

The Snake Task lasts approximately 1.5 minutes, and has been previously shown to induce anxiety and fear in children [19], [20]. The task was temporally segmented into three threat response phases:

1. Potential Threat

   When entering a novel, dimly lit room, the administrator whispers to the child, "There's something I want to show you in this room." The administrator then slowly steps forward into the middle of the room, gesturing the child to stand still in front of a covered terrarium. The administrator whispers, "I'm going to uncover it now" and steps toward the terrarium.

2. Startle

The administrator quickly uncovers the terrarium and pulls the fake snake out toward the child at their eye level. The administrator then says, “See it’s fake, you can touch it”.

3. Response Modulation

   The administrator continues holding the snake for the child to see, reassures verbally as needed (e.g., “It’s just a silly toy snake.”), and waits in the room before gesturing the child to leave the room with them.

After the Snake Task, children transitioned to free play with the administrator to regulate and debrief about their experience.

D. Questionnaires

The Child Behavior Checklist 1.5–5 and 6–18 (CBCL) [21] was used to assess internalizing symptoms. Symptoms include anxious and depressed problems (e.g., “fearful”, “feels worthless”), withdrawn and depressed problems (e.g., “sad”, “lacks energy”), and somatic complaints (e.g., “nightmares”, “overtired”). Internalizing broadband scores were standardized into ‘T scores’ respective to child age and sex. No child met the threshold T score of 70 which would indicate a clinical disorder.

PTSD was assessed using the National Women’s Study PTSD Module [22], which yields a score related to the number and severity of symptoms caused by a traumatic event (continuous scale, 0–17). This score is an aggregate measure of symptoms clustered into three categories: Re-experiencing (e.g., flashbacks/nightmares of the event), Hyper-arousal (e.g., insomnia, exaggerated startle response), and Avoidance (e.g., efforts to avoid reminders of trauma, detachment).

E. Instrumentation and Data Processing

Motion of each participant was tracked using a belt-worn inertial measurement unit (3–Space Sensor, YEI Technology, Portsmouth, OH, USA). Measurements from the accelerometer and angular rate gyro of the IMU are defined as $\vec{a}_M$ and $\vec{\omega}_M$, respectively. The angular rate gyro measurements can be modeled as a linear combination of the angular velocity ($\vec{\omega}$), a time-varying bias ($\vec{\omega}_b$), and white measurement noise ($\vec{n}_\omega$) as per

$$\vec{\omega}_M = \vec{\omega} + \vec{\omega}_b + \vec{n}_\omega \quad (1)$$

Similarly, the accelerometer data can be modeled as a linear combination of translational acceleration ($\vec{a}$), the acceleration due to gravity ($\vec{g}$), and white measurement noise ($\vec{n}_a$) as per

$$\vec{a}_M = \vec{a} + \vec{g} + \vec{n}_a \quad (2)$$

These values are reported in a body-fixed frame F_M characterized by the orthonormal vector triad ($\hat{x}_M$, $\hat{y}_M$, $\hat{z}_M$, see Fig. 1) and assumed to be roughly aligned with the anatomical axes

of the body (Anterior-Posterior : $\hat{z}_M$, Medial-Lateral : $\hat{x}_M$, Longitudinal : $\hat{y}_M$). Data were sampled by the device at approximately 300 Hz, down-sampled to 100 Hz, and low pass filtered using a 4th order Butterworth IIR filter with a cutoff frequency of 20 Hz in software prior to use.

To help quantify the motion of each participant, we define an inertial frame F_G characterized by the orthonormal vector triad ($\hat{x}_G$, $\hat{y}_G$, $\hat{z}_G$, see Fig. 1) where $\hat{z}_G$ is aligned with gravity. The quaternion ($\vec{q}$) defining the relationship between F_G and F_M is calculated following the complementary filtering technique described in [23] and evolves from a short period of time at the beginning of the task where each participant was asked to stand still. This initial condition enables numerical solution of the system of ordinary differential equations that describe the evolution of the angular rate gyro bias and quaternion, respectively, as per

$$\dot{\vec{\omega}}_b = -K_I \vec{\theta} \quad (3)$$

$$\dot{\vec{q}} = \frac{1}{2} \vec{q} \otimes \vec{q}_{\vec{\omega}'} \quad (4)$$

where K_I is an adaptive gain, $\vec{\theta}$ is a time-varying error term that captures the angular difference between the direction of gravity identified with each data source, $\otimes$ refers to the quaternion multiplication operation, and $\vec{q}_{\vec{\omega}'}$ is the quaternion representation of the estimated angular velocity. This angular velocity is defined as

$$\vec{\omega}' = \vec{\omega}_M - \vec{\omega}_b + K_P \vec{\theta} \quad (5)$$

where K_P is an adaptive gain, and the quaternion representation of $\vec{\omega}' = \omega'_x \hat{x}_M + \omega'_y \hat{y}_M + \omega'_z \hat{z}_M +$ is defined as

$$\vec{q}_{\vec{\omega}'} = \mathbf{0} + \left(\omega'_x \hat{x}_M + \omega'_y \hat{y}_M + \omega'_z \hat{z}_M \right) \quad (6)$$

Fundamentally, the complementary filtering algorithm described in (3)–(5) fuses error-prone orientation estimates from the accelerometer and angular rate gyro to yield an accurate orientation estimate with bounded error. Additional details regarding this approach are presented in [23].

The resulting quaternion is used to resolve the measured acceleration and angular velocity in F_G as per

$$\vec{q}_G = \vec{q} \otimes \vec{q}_M \otimes \vec{q}^* \quad (7)$$

where $\vec{q}^*$ is the conjugate[1] of $\vec{q}$, and $\vec{q}_M$ and $\vec{q}_G$ are quaternion representations of vectors resolved in F_M and F_G, respectively. Accelerometer and angular rate gyro measurements resolved in F_G are defined as $\vec{a}_G$ and $\vec{\omega}_G$, respectively. The translational acceleration of the participant, sampled at the location of the IMU and resolved in F_G, is then defined as

$$\vec{d} = \vec{d}_G - g\,\hat{z}_G \quad (8)$$

where $\vec{a}$ is the translational acceleration and $g = 9.81$ m/s^2.

F. Data Segmentation

The approximate startle instant was identified manually in a video recording of the task for each participant and the corresponding point was then identified in the inertial sensor data. The IMU data was aligned with the video using several synchronization events including participant transitions from resting to moving. As indicated in Fig. 2, the startle period was defined as the six seconds immediately surrounding the identified startle instant (three seconds before and three seconds after). The potential threat and response modulation periods were then defined as the 20 seconds immediately before and after the start and end of the startle period, respectively.

G. Movement Indicators

Data from the IMU were used to calculate a series of six movement indicators for each analysis period. Calculation of these quantities begins by defining the vertical component and horizontal magnitude of the acceleration and angular velocity as per

$$a_V = \vec{d} \cdot \hat{z}_G \quad (9)$$

$$a_H = \| \vec{d} - a_V \cdot \hat{z}_G \|_2 \quad (10)$$

$$\omega_V = \vec{\omega} \cdot \hat{z}_G \quad (11)$$

[1]For $\vec{q} = q_0 + q_1\,\hat{x}_M + q_2\,\hat{y}_M + q_3\,\hat{z}_M$, the quaternion conjugate $\vec{q}^* = q_0 - q_1\,\hat{x}_M - q_2\,\hat{y}_M - q_3\,\hat{z}_M$

$$\omega_H = \| \vec{\omega} - \omega_V \cdot \hat{z}_G \|_2 \quad (12)$$

where a_V and a_H are the vertical component and horizontal magnitude of the translational acceleration, respectively, and ω_V and ω_H are the corresponding angular velocity quantities. These quantities represent time series during each threat response phases. We reduce dimensionality by taking the root mean square (rms) of each time series during each phase. The horizontal and vertical acceleration movement indicators are then defined as ah_{rms}^{PT}, ah_{rms}^{S}, ah_{rms}^{RM}, av_{rms}^{PT}, av_{rms}^{S}, and av_{rms}^{RM} during potential threat, startle, and response modulation, respectively. Similarly, the horizontal and vertical angular velocity movement indicators are defined as ωh_{rms}^{PT}, ωh_{rms}^{S}, ωh_{rms}^{RM}, ωv_{rms}^{PT}, ωv_{rms}^{S}, and ωv_{rms}^{RM} during potential threat, startle, and response modulation, respectively.

The next series of movement indicators are based on the tilt angle (α), which is an approximate measure of the tilt of the subject's waist/torso from vertical. This quantity is defined as the angle between $\hat{y}_M$ and $\hat{z}_G$ at every instant during the task, and is calculated as per

$$\alpha = \cos^{-1}(R(\hat{y}_M) \cdot \hat{z}_G) \quad (13)$$

where $R(\cdot)$ is a rotation operator that transforms a vector resolved in F_M to F_G as per (7). We define the tilt angle movement indicator as the range of α during the corresponding threat response phase, where α_{rom}^{PT}, α_{rom}^{S}, and α_{rom}^{RM} are the tilt range of motion (rom) during potential threat, startle, and response modulation, respectively. The final series of movement indicators are based on the yaw angle (γ), which is an approximate measure of the direction the subject's waist/torso is pointing within the plane of the floor. The yaw angle is calculated by considering the projection of $\hat{z}_M$ onto the horizontal plane as per

$$\hat{z}_{Mproj} = \frac{R(\hat{z}_M) - (R(\hat{z}_M) \cdot \hat{z}_G)\hat{z}_G}{\| R(\hat{z}_M) - (R(\hat{z}_M) \cdot \hat{z}_G)\hat{z}_G \|_2} \quad (14)$$

The yaw angle is then defined as the angle between the current ($\hat{z}_{Mproj}$) and initial ($\hat{z}_{Mproj}(0)$) projection of $\hat{z}_M$ onto the horizontal plane as per

$$\gamma = \cos^{-1}\left(\hat{z}_{Mproj} \cdot \hat{z}_{Mproj}(0)\right) \quad (15)$$

We define the yaw angle movement indicator as the range of γ during the corresponding threat response phase, where γ_{rom}^{PT}, γ_{rom}^{S}, and γ_{rom}^{RM} are the yaw rom during potential threat, startle, and response modulation, respectively.

H. Statistical Analysis

Descriptive statistics including means, kurtosis, and skewness were calculated on the six movement indicators across the three phases, as well as familial PTSD symptoms and child internalizing symptoms (see Table I). All variables met normal assumptions with the exception of ah_{rms}^{S} (kurtosis 3.41, SE 1.04) and ωh_{rms}^{RM} (kurtosis 3.27, SE 1.04), which were corrected after being log transformed. Movement indicators were correlated across phases, familial PTSD symptoms, and child symptoms. Significance for all analyses were interpreted at $p < 0.05$.

III. Results

In addition to the descriptive statistics reported in Table I, tables show results of bi-variate correlation matrices for Inter-correlated Motions (Table II), and Motions by Child Anxiety Risks (Table III).

IV. Discussion

The measures extracted from IMU data for each subject provide unique insight into each participant's distinct movements. Specifically, the horizontal and vertical acceleration rms measures indicate the intensity of translational motion in the horizontal plane and vertical direction, respectively. Similarly, the horizontal and vertical angular velocity rms measures indicate how fast a subject is leaning forward and backward (and left and right although this behavior was less common in the study sample). The tilt and yaw rom measures indicate how far each participant leans forward and backward and turns left and right, respectively. Motion during potential threat was procedurally characterized by slow approach to an unknown stimulus, so the associated movement indicators provide context for interpretation of subsequent, more abrupt movement in the startle and response modulation phases. Based on the data reported in Table I, the horizontal and vertical acceleration measures during startle are 2–3x those during potential threat (mean $ah_{rms}^{S}=3.23\,\mathrm{m/s^2}$ vs. $ah_{rms}^{PT}=1.41\,\mathrm{m/s^2}$ and $av_{rms}^{S}=2.76\,\mathrm{m/s^2}$ vs. $av_{rms}^{PT}=1.18\,\mathrm{m/s^2}$), and with significantly increased variability across the sample (standard deviation $ah_{rms}^{S}=3.03\,\mathrm{m/s^2}$ vs. $ah_{rms}^{PT}=0.91\,\mathrm{m/s^2}$ and $av_{rms}^{S}=2.38\,\mathrm{m/s^2}$ vs. $av_{rms}^{PT}=0.97\,\mathrm{m/s^2}$), indicating that the acute threat introduced during startle yielded a substantial and varied change in participant behavior.

The correlations reported in Table II demonstrate that there is carryover between startle and response modulation, where subjects who exhibit higher motion intensity (ah_{rms}^{S}, av_{rms}^{S}) and leaning/turning speed (ωh_{rms}^{S}, ωv_{rms}^{S}) during startle exhibit similar behavior during response modulation, as evidenced by the significant, positive correlations. This suggests that the 20-second duration response modulation phase may be too short for participants with the largest physical reactions to acute threat to return to a behavioral baseline. Similarly, participants with the largest yaw rom during startle (γ_{rom}^{S}) exhibit higher motion intensities (ah_{rms}^{S}, av_{rms}^{S}) during response modulation, as evidenced by significant, positive correlations. This movement pattern suggests that participants who respond to the acute

threat by turning their body (maximizing yaw rom) follow this reaction by then quickly moving away during the response modulation phase.

Interestingly, child anxiety risk factors as characterized by familial PTSD symptoms (total score and/or symptom clusters), were significantly *negatively* associated with potential threat motion (less leaning (ωh_{rms}^{PT}) and turning (ωv_{rms}^{PT}) speed, less horizontal motion intensity (ah_{rms}^{S})), but significantly *positively* associated with response modulation motion (more leaning (ωh_{rms}^{RM}) and turning (ωv_{rms}^{RM}) speed, larger turning range of motion (γ_{rom}^{RM})). These differential correlations demonstrate the sensitivity of this technology to these constructs, while connecting them to familial PTSD symptoms in directions consistent with prior research (i.e., freezing behaviors in response to potential threat [24]; emotional dysregulation in the face of acute threat [25]).

Child internalizing symptoms were significantly related to startle turning range of motion (γ_{rom}^{S}), such that children were turning their entire body away from the trigger (γ_{rom}^{S} nearly 180 deg.), and thus effectively avoiding the threat, in the three seconds post reveal. This motion, and timing, suggests a heightened physiological reactivity to acute threat, supporting previous FPS work demonstrating that children with internalizing risk have a more pronounced eye blink startle response (shutting their eyes in a defensive reflex) in the moments post reveal [7]–[9]. The immediate nature of this heightened startle reactivity suggests that the child's own internalizing symptoms may represent a biological/physiological sensitivity to acute threat. In contrast, correlations between variables within the Potential Threat or Response Modulation phases with familial PTSD may suggest learned environmental attunement from modeled parental behaviors. Moving forward, movement indicators extracted from IMU data during the 6-second startle period could be validated as an alternative, more feasible method for examining startle response.

More broadly, these results demonstrate the efficacy of this 2-minute startle task, meant to press for indicators of emerging psychopathology that are not readily observable during ordinary circumstances. While startle tasks are commonly used in child research, and present only minimal risk to participants, it is important to ensure that children are given the opportunity to debrief and discuss any induced anxiety following the task. In the current study, we address this concern in two ways. First, during the lab visit, participants engaged in positive mood induction tasks in addition to the anxiety inducing startle task, in an effort to present a balanced range of emotional expression. Second, following the startle task, administrators briefly discussed the child's experience with them and validated their expressed emotions in an effort to aid child startle recovery. While there was no immediate benefit for participants besides compensation/toy gifts, parents and children were informed that this research could help future children by improving clinical assessment, and that induced anxiety plays a pivotal role in accomplishing this objective.

Future studies should increase sample size and compare motion results with FPS eye blink outcomes, coded child anxiety/fear behaviors, and other indicators of child anxiety risk. Nevertheless, the results presented herein demonstrate that an IMU can be used for measuring child motion quickly and inexpensively during clinical mood induction tasks, and

that these measurements correlate with risk for developing mood and anxiety disorders. This is especially salient as these young patients are unable to effectively self-report their emotional needs [3], which often prevents early detection of risk. It is important to identify risk early as it improves the efficacy of prevention and intervention efforts [2]. In sum, this indicates the promise of this technology as a supplemental behavioral assessment tool for anxiety and mood disorders in clinical research and practice, and at a small fraction of the cost, time, and effort associated with existing techniques (i.e. FPS, behavioral coding).

V. Conclusion

In this proof of concept study, we characterized the movements of young children during a fear induction task using a belt-worn IMU. We demonstrate that this technology, and the extracted movement parameters, provides sufficient sensitivity to discriminate the temporal constructs of potential threat, startle to acute threat, and response modulation following threat in a sample of children with heightened risk for anxiety.

Acknowledgments

This work was supported in part by NIMH K23-MH080147 (PI: Muzik); Michigan Institute for Clinical and Health Research (UL1TR000433, PI: Muzik; Biomedical and Social Sciences Scholar Program PI: E.W. McGinnis); Blue Cross Blue Shield of Michigan Foundation Grant (1982.SAP, PI: E.W. McGinnis); Brain Behavior Research Foundation (PI: Fitzgerald); NIMH R03MH102648 (PI: Fitzgerald; Rosenblum).

References

1. Cartwright-Hatton S, McNicol K, Doubleday E. Anxiety in a neglected population: prevalence of anxiety disorders in pre-adolescent children. Clin Psychol Rev. Nov; 2006 26(7):817–833. [PubMed: 16517038]
2. Luby JL. Preschool Depression: The Importance of Identification of Depression Early in Development. Curr Dir Psychol Sci. May; 2010 19(2):91–95. [PubMed: 21969769]
3. Garber J, Kaminski KM. Laboratory and performance-based measures of depression in children and adolescents. J Clin Child Psychol. Dec; 2000 29(4):509–525. [PubMed: 11126630]
4. Kolko DJ, Kazdin AE. Emotional/behavioral problems in clinic and nonclinic children: correspondence among child, parent and teacher reports. J Child Psychol Psychiatry. Sep; 1993 34(6):991–1006. [PubMed: 8408380]
5. National Institute of Mental Health (NIMH). NIMH Research Domain Criteria (RDoC).
6. Gross JJ. Emotion regulation: affective, cognitive, and social consequences. Psychophysiology. May; 2002 39(3):281–291. [PubMed: 12212647]
7. Waters AM, Craske MG, Bergman RL, Naliboff BD, Negoro H, Ornitz EM. Developmental changes in startle reactivity in school-age children at risk for and with actual anxiety disorder. Int J Psychophysiol Off J Int Organ Psychophysiol. Dec; 2008 70(3):158–164.
8. Kujawa A, Glenn CR, Hajcak G, Klein DN. Affective modulation of the startle response among children at high and low risk for anxiety disorders. Psychol Med. Sep; 2015 45(12):2647–2656. [PubMed: 25913397]
9. Bakker MJ, Tijssen MAJ, van der Meer JN, Koelman JHTM, Boer F. Increased whole-body auditory startle reflex and autonomic reactivity in children with anxiety disorders. J Psychiatry Neurosci JPN. Jul; 2009 34(4):314–322. [PubMed: 19568483]
10. Vasey MW, Lonigan CJ. Considering the clinical utility of performance-based measures of childhood anxiety. J Clin Child Psychol. 2000; 29(4):493–508. [PubMed: 11126629]
11. Gagne JR, Van Hulle CA, Aksan N, Essex MJ, Goldsmith HH. Deriving childhood temperament measures from emotion-eliciting behavioral episodes: Scale construction and initial validation. Psychol Assess. 2011; 23(2):337. [PubMed: 21480723]

12. Durbin CE. Validity of young children's self-reports of their emotion in response to structured laboratory tasks. Emot Wash DC. Aug; 2010 10(4):519–535.
13. Olino TM, Klein DN, Dyson MW, Rose SA, Durbin CE. Temperamental emotionality in preschool-aged children and depressive disorders in parents: associations in a large community sample. J Abnorm Psychol. Aug; 2010 119(3):468–478. [PubMed: 20677836]
14. Moser JS, Durbin CE, Patrick CJ, Schmidt NB. Combining Neural and Behavioral Indicators in the Assessment of Internalizing Psychopathology in Children and Adolescents. J Clin Child Adolesc Psychol Off J Soc Clin Child Adolesc Psychol Am Psychol Assoc Div. Jan.2014 53
15. McGinnis RS, Cain SM, Tao S, Whiteside D, Goulet GC, Gardner EC, Bedi A, Perkins NC. Accuracy of Femur Angles Estimated by IMUs During Clinical Procedures Used to Diagnose Femoroacetabular Impingement. IEEE Trans Biomed Eng. Jun; 2015 62(6):1503–1513. [PubMed: 25608299]
16. McGinnis R, Cain S, Davidson S, Vitali R, Perkins N, McLean S. Quantifying the Effects of Load Carriage and Fatigue under Load on Sacral Kinematics during Countermovement Vertical Jump with IMU-based Method. Sports Eng. 2015
17. Yehuda R, Schmeidler J, Wainberg M, Binder-Brynes K, Duvdevani T. Vulnerability to posttraumatic stress disorder in adult offspring of Holocaust survivors. Am J Psychiatry. Sep; 1998 155(9):1163–1171. [PubMed: 9734537]
18. Mesman J, Koot HM. Early preschool predictors of preadolescent internalizing and externalizing DSM-IV diagnoses. J Am Acad Child Adolesc Psychiatry. Sep; 2001 40(9):1029–1036. [PubMed: 11556626]
19. Calkins SD, Graziano PA, Berdan LE, Keane SP, Degnan KA. Predicting cardiac vagal regulation in early childhood from maternal-child relationship quality during toddlerhood. Dev Psychobiol. Dec; 2008 50(8):751–766. [PubMed: 18814182]
20. Lopez-Duran NL, Hajal NJ, Olson SL, Felt BT, Vazquez DM. Individual differences in cortisol responses to fear and frustration during middle childhood. J Exp Child Psychol. Jul; 2009 103(3): 285–295. [PubMed: 19410263]
21. Achenbach TM, Rescorla LA. ASEBA School Age Forms and Profiles. Burlingt Vt ASEBA. 2001
22. Resnick HS, Kilpatrick DG, Dansky BS, Saunders BE, Best CL. Prevalence of civilian trauma and posttraumatic stress disorder in a representative national sample of women. J Consult Clin Psychol. Dec; 1993 61(6):984–991. [PubMed: 8113499]
23. McGinnis, R., Cain, S., Davidson, S., Vitali, R., McLean, S., Perkins, N. Validation of Complementary Filter Based IMU Data Fusion for Tracking Torso Angle and Rifle Orientation. Proceedings of ASME 2014 International Mechanical Engineering Congress and Exposition; Montreal, QC. 2014. vol. In Press
24. Adenauer H, Catani C, Keil J, Aichinger H, Neuner F. Is freezing an adaptive reaction to threat? Evidence from heart rate reactivity to emotional pictures in victims of war and torture. Psychophysiology. Mar; 2010 47(2):315–322. [PubMed: 20030756]
25. Schechter DS, Coots T, Zeanah CH, Davies M, Coates SW, Trabka KA, Marshall RD, Liebowitz MR, Myers MM. Maternal mental representations of the child in an inner-city clinical sample: violence-related posttraumatic stress and reflective functioning. Attach Hum Dev. Sep; 2005 7(3): 313–331. [PubMed: 16210242]

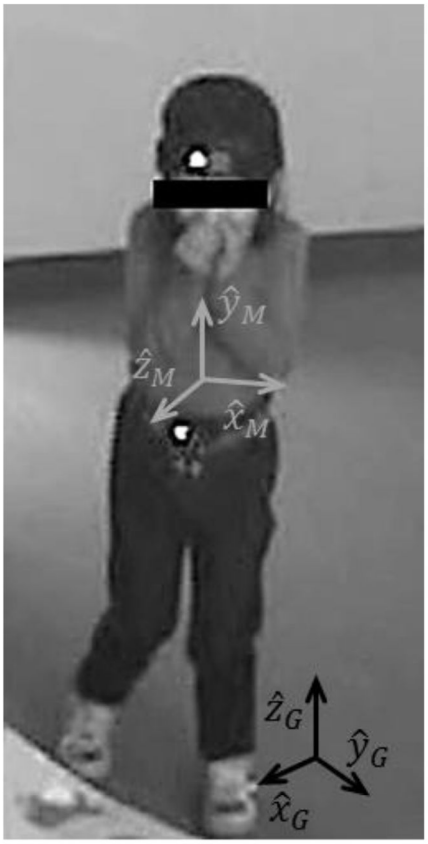

Fig. 1.

Belt worn IMU secured to participant. Body-fixed device measurement frame (F_M) and ground-fixed inertial frame (F_G) are as illustrated.

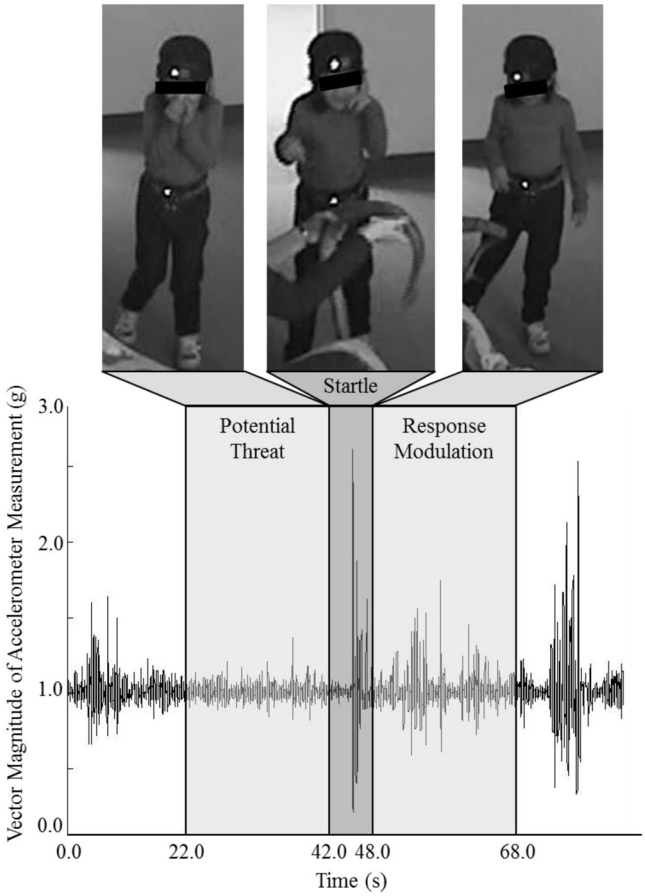

Fig. 2.

Vector magnitude of accelerometer measurement with the potential threat, startle, and response modulation periods (and corresponding images) indicated.

TABLE I

Descriptive Statistics for Child Motion and Familial and Child Anxiety Risk Factors

Measure (Units)	Range	Mean (SD)
ah_{rms}^{PT} (m/s^2)	0.60–3.91	1.41 (0.91)
av_{rms}^{PT} (m/s^2)	0.39–3.38	1.18 (0.97)
α_{rom}^{PT} (deg)	10.52–82.72	27.87 (19.81)
γ_{rom}^{PT} (deg)	42.49–179.98	99.15 (44.89)
ωh_{rms}^{PT} (deg/s)	12.05–56.45	26.96 (12.71)
ωv_{rms}^{PT} (deg/s)	13.13–70.07	35.65 (16.72)
ah_{rms}^{S} (m/s^2)	0.30–11.84	3.23 (3.03)
av_{rms}^{S} (m/s^2)	0.25–7.25	2.76 (2.38)
α_{rom}^{S} (deg)	1.97–32.26	16.69 (10.25)
γ_{rom}^{S} (deg)	1.16–179.79	86.30 (60.00)
ωh_{rms}^{S} (deg/s)	1.79–170.80	65.99 (54.71)
ωv_{rms}^{S} (deg/s)	1.20–198.79	60.42 (47.96)
ah_{rms}^{RM} (m/s^2)	0.47–4.77	1.72 (1.24)
av_{rms}^{RM} (m/s^2)	0.35–4.73	1.48 (1.23)
α_{rom}^{RM} (deg)	8.15–59.20	23.49 (14.75)
γ_{rom}^{RM} (deg)	20.03–179.98	108.08 (56.26)
ωh_{rms}^{RM} (deg/s)	6.98–130.16	35.69 (32.43)
ωv_{rms}^{RM} (deg/s)	13.50–74.61	37.14 (19.58)
Familial PTSD Symptoms	0–12	5.65 (3.59)
Re–experiencing Symptoms	0–4	1.35 (1.11)
Avoidance Symptoms	0–4	1.88 (1.62)
Hyper-arousal Symptoms	0–5	2.41 (1.54)
Internalizing Symptoms	33–69	44.75 (9.54)

TABLE II

Bi-Variate Correlation Matrix of Motion Factors in startle and Response Modulation Phases (N=18)

	ah^{RM}_{rms}	av^{RM}_{rms}	α^{RM}_{rom}	γ^{RM}_{rom}	$\omega h^{RM}_{rms}\boldsymbol{L}$	ωv^{RM}_{rms}
$ah^{S}_{rms}L$	**.667**	**.685**	.336	.415^{t}	**.554**	.550
av^{S}_{rms}	**.705**	**.738**	.388	.415^{t}	**.555**	**.514**
α^{S}_{rom}	.380	.306	.461^{t}	.445^{t}	.388	.317
γ^{S}_{rom}	**.503**	**.493**	.257	.238	.238	.310
ωh^{S}_{rms}	**.673**	**.714**	.455^{t}	.353	**.636**	**.524**
ωv^{S}_{rms}	**.675**	**.685**	.195	.399^{t}	**.466**	**.521**

Note: Bold indicates p<0.05,

^{t}indicates trend at p<0.10,

^{L}indicates variable is log transformed

TABLE III

Bi-Variate Correlation Matrix of Motion Factors by Child Anxiety Risk Factors

	Familial PTSD Symptoms (n=17)				Child Symptoms (n=16)
Motion	**Total PTSD**	**Re-experiencing**	**Avoidance**	**Hyper-arousal**	**Internalizing**
ah_{rms}^{PT}	−.363	.421^{t}	−.051	**−.487**	−.001
av_{rms}^{PT}	.227	−.359	.044	−.314	−.138
α_{rom}^{PT}	.210	.065	.396	.026	−.150
γ_{rom}^{PT}	−.290	−.337	−.135	−.288	.481^{t}
ωh_{rms}^{PT}	−.246	**−.451**	.076	−.325	−.136
ωv_{rms}^{PT}	−.399	**−.519**	−.067	**−.484**	.26
$ah_{rms}^{S}{}_{L}$	.293	.187	.251	.282	.347
av_{rms}^{S}	.145	.059	.272	.009	.303
α_{rom}^{S}	.230	.226	.147	.216	−.052
γ_{rom}^{S}	.032	−.123	.145	.012	**.512**
ωh_{rms}^{S}	.110	.095	.181	−.001	.361
ωv_{rms}^{S}	.260	.126	.362	.113	.248
ah_{rms}^{RM}	.277	.186	.417^{t}	.072	.496^{t}
av_{rms}^{RM}	.366	.306	.477^{t}	.131	.459^{t}
α_{rom}^{RM}	.249	.294	.291	.061	.385

IEEE J Biomed Health Inform. Author manuscript; available in PMC 2017 September 07.

	Familial PTSD Symptoms (n=17)				Child Symptoms (n=16)
Motion	**Total PTSD**	**Re-experiencing**	**Avoidance**	**Hyper-arousal**	**Internalizing**
γ_{rom}^{RM}	**.554**	.473[t]	**.543**	.379	.320
$\omega h_{rms}^{RM}{}_{L}$	.449[t]	**.564**	.374	.245	.361
ωv_{rms}^{RM}	**.424**	.446[t]	.350	.297	.399

Note: Bold indicates $p<0.05$,

[t] indicates trend at $p<0.10$,

[L] indicates variable is log transformed.